

# Evaluation of Solar Reference Cells on a Two-Axis Tracker Using Spectral Measurements

Frank Vignola<sup>1, a)</sup>, Josh Peterson<sup>1</sup>, Rich Kessler<sup>1</sup>, Sean Snider<sup>2</sup>, Afshin Andreas<sup>3</sup>, Aron Habte<sup>3</sup>, Peter Gotseff<sup>3</sup>, Manajit Sengupta<sup>3</sup>, Fotis Mavromatakis<sup>4</sup>

<sup>1</sup>Material Science Institute, 1252 – University of Oregon, Eugene, Oregon 97403-1252, USA

<sup>2</sup>Saint Mary's High School, 816 Black Oak Dr., Medford, Oregon 97504, USA

<sup>3</sup>National Renewable Energy Laboratory, 15013 Denver West Parkway, Golden, Colorado 80401, USA

<sup>4</sup>Department of Electrical and Computer Engineering, Hellenic Mediterranean University, 71410 Estavromenos, Heraklion, Crete, Greece

<sup>a)</sup>Corresponding author: Frank Vignola: [fev@uoregon.edu](mailto:fev@uoregon.edu)

<sup>b)</sup>Josh Peterson: [jpeter4@uoregon.edu](mailto:jpeter4@uoregon.edu)

**Abstract.** A simple model calculating the performance of an IMT solar reference cell is proposed and tested under clear sky periods. One-minute data from EKO spectroradiometers collocated with an IMT reference cell are used for the analysis. Data are obtained at the NREL Solar Radiation Research Laboratory in Golden, Colorado and the UO Solar Radiation Monitoring Laboratory in Eugene, Oregon. The model is also applied and evaluated under cloudy conditions. A match of better than 1% is found between calculated clear sky values and IMT measurements for July, 2020. One-minute cloudy sky comparisons show a much larger variation, but when averaged over one hour, a standard deviation of 4% between the calculated and measured values is found.

## INTRODUCTION

Reference cells are used for many tasks ranging from testing of photovoltaic (PV) modules on the production line to monitoring system performance in the field. Reference cells are designed to mimic many of the characteristic of PV modules. Reference cells are not designed to measure incident radiation. An issue arises when trying to use reference measurements in place of pyranometers are measurement of the incident radiation. Compared to high quality pyranometers, reference cells exhibit large systematic biases that can skew calculations requiring accurate irradiance values.

Typically reference cells use the same solar cell technology and encapsulant as the PV modules they monitor. Besides size, the biggest difference between reference cells is that they operate at short circuit current while PV modules operate at the max power point. Because reference cells use solar cells, they are sensitive to the incident spectral radiation and the glazing and encapsulant result in a pronounced angle-of-incident (AOI) effect especially at large incident angles.

A standard method to evaluate the field performance of reference cells is to compare reference cells directly to the performance of high-quality pyranometers. A plot of the ratio of the IMT reference cell to a CMP22 pyranometer on a two axis tracker during clear periods is shown in Fig. 1 during the morning of May 3, 2020 and the afternoon on May 4, 2020. Two factors clearly add to the deviation of the curves from a straight line. First and largest is that the reference has a significant dependence on the spectral distribution of the incident radiation. The angle-of-incident affects are minimal since both are on a two-axis tracker pointed directly towards the sun. The pyranometer is calibrated for a range of incident angle from 30° to 60° while the reference cell is typically calibrated with an AOI of 0°. While taking into account the spectral differences can push the two curves closer together, the magnitude of the difference from 1 is somewhat related to the calibration differences between the two instruments (See Fig. 2). More information on setting standards for reference cell evaluations can be found in [1].

Previous approaches for evaluating the reference cell with respect to a reference pyranometer revealed that several factors that must be taken into account complicating the analysis [2, 3, 4, and 5]. The purpose of this paper is to report some initial finding of the performance of a reference mono-silicon reference cell on a two-axis tracker with co-mounted spectroradiometers, reference cells, and a high-quality reference pyranometer. The experimental setup is first described. The method used to analyze and model the performance of the reference cell is then detailed. A simplifying assumption is made to asset in the analysis and the rational for this assumption is discussed. Next the ratio of the IMT measurements to calculated IMT values is examined under clear skies. Because of the limited time the experiment has been running, only July data will be utilized. As more data becomes available, the comparisons with other periods will be made. For any firm conclusions at least a year of data are needed.

Cloudy and partially cloudy skies present a much more challenging problem and the cloudy periods in July are studied for comparison. A brief discussion of the findings are then presenting in this section. At the end, a summary of the finding are discussed and the paper ends with a description of future activities as more data becomes available.

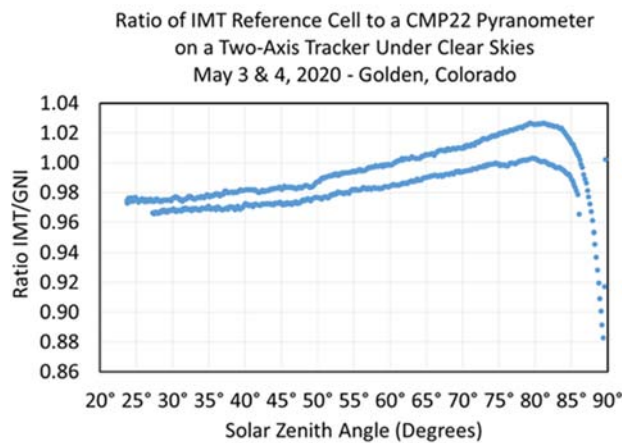


**FIGURE 1.** Ratio of the IMT reference cell to a CMP22 pyranometer measurement on a two-axis tracker at NREL’s SRRL in Golden, Colorado on the morning of May 3, 2020 and the afternoon of May 4, 2020.

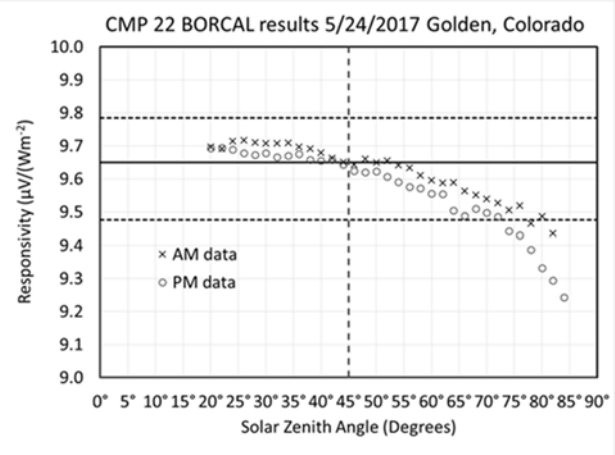


**FIGURE 2.** BORCAL evaluation of a CMP22 pyranometer used at SRRL. The responsivity of this pyranometer from 30° to 60° is 9.650 +1.4% -1.8% with a 95% confidence level.

## EXPERIMENTAL SETUP

The National Renewable Energy Laboratory (NREL) at its Solar Resource Research Laboratory (SRRL) and the University of Oregon Solar Radiation Monitoring Laboratory (UO SRML) have installed two-axis EKO trackers to monitor the performance of several reference cells. Currently each station is equipped with four reference silicon cells, Li-Cor 200R and Kipp & Zonen SP Lite2 pyranometers, Kipp & Zonen CMP22 pyranometer, and EKO spectroradiometer(s). The number of reference cells will be increased to evaluate different technologies. The two spectroradiometers at SRRL measure spectral radiation from 300 nm – 1650 nm and the EKO spectroradiometer in Eugene measures irradiance from 300 nm – 1100 nm. In addition, there are additional equipment in Golden, Colorado at SRRL that have instruments on a one-axis tracker, a fix tilt, and on a horizontal surface. In Eugene are the UO SRML, there are instruments on a horizontal surface. Data from these instruments have been used in earlier studies [2-5] and can provide test of results from the current study when it is completed.

The experimental setup at SRRL is shown in Fig. 3. The two EKO spectroradiometers are shown by the blue arrows. The IMT reference cell highlighted in this study is shown by the red arrow. The other three reference cells are shown by the green arrows. The CMP22 reference pyranometer is shown with the yellow arrow.

Data collection on the two-axis tracker started in May 2020 at SRRL and in June 2020 at the UO SRML. All data are reported in one-minute intervals. The spectral data takes from 0.1 to 5 seconds to gather and are stored at the top of the minute. All other instruments are scanned once every three seconds and the average measurement is recorded

at the ending time. This time difference isn't significant under clear skies but makes it hard to use the spectral data under cloudy or partially cloudy skies. This will be covered more in the section on cloudy skies.



FIGURE 3. Experimental equipment at SRRL in Golden, Colorado.

## MODELING REFERENCE CELL OUTPUT WITH SPECTRAL AND TEMPERATURE DATA

Reference cells use solar cells that have a spectral responsivity [2-5]. The output of reference cells are dependent on the spectral distribution of the incident radiation. In addition, the output of the reference cell is directly proportional to the irradiance making it through the glazing. On a two-axis tracker, light coming directly from the sun passes through this glazing without noticeable reduction. Diffuse and ground reflected radiation are incident from many directions and a portion of this scatter radiation is reflected or doesn't make it through the glazing. Because the variety of directions and the variation of scattered irradiance across the sky, the scattered contribution to the radiation incident on the solar cell has to be modeled.

Because of the complexity of the incident radiation under cloudy or partially cloudy skies, this analysis is broken into two sections. First the clear sky performance will be discussed. This will be followed by examining what happens under cloudy or partially cloudy conditions.

A simple model for the output of a reference cell ( $RC_{Model}$ ) is given in Eq. 1.

$$RC_{Model} = K \cdot \int R_{\lambda} \cdot I_{\lambda} \cdot T_{\lambda} \cdot (T_{rc} - 25^{\circ}C) \cdot F(AOI) \cdot d\lambda \quad Eq. 1$$

where  $R_{\lambda}$  is the spectral responsivity of the reference cell obtained from the normalized percent quantum efficiency and  $K$  is a calibration constant that turns the measured Amps to  $Wm^{-2}$ . The irradiance is  $I_{\lambda}$ , the spectral temperature dependence is  $T_{\lambda}$ ,  $T_{rc}$  is the reference cell temperature, and  $F(AOI)$  is the dependence on the angle-of-incidence. The integral is over all wavelengths, but in practice it is over 300 nm – 1249 nm. The spectral responsivity for the IMT reference cell is zero outside this range.

For this study, the sum over all wavelengths replaces the integral. In this case the one-minute interval spectral data is given for each integer wavelength in the 300 nm – 1249 nm range. If the wavelength data has a different spacing, that spacing has to be taken into account.

### Simplifying the Model

A discussion of  $R_{\lambda}$  and  $T_{\lambda}$  are available in earlier work [3 – 5]. The spectral response,  $R_{\lambda}$ , is obtained from the Quantum Efficiency (QE) values measured by the NREL PV Characterization group in a laboratory using a solar simulator maintained and operated in accordance with the ASTM E1021 standards (<https://www.astm.org/Standards/E1021.htm>).  $T_{\lambda}$  is determined from measuring  $R_{\lambda}$  at different temperatures.

Normally the temperature dependence for a reference cell is calculated on average change with temperature and is around 0.0008 per °C.

The angle-of-incidence transmission through the glazing,  $F(AOI)$ , varies with wavelength, but this variation is small for the wavelengths relevant to reference cells. For  $RC_{Model}$  it is assumed independent of wavelength. In addition,  $F(AOI)$  determined using Snell's Law and presented in [6] is used for estimating the transmission of light at all wavelengths. Since the instruments are mounted on a two-axis tracker that points to the sun, an  $F(AOI) = 1$  is assumed. Actually the direct normal irradiance (DNI) constitutes 80% to 90% of the total irradiance incident on a two-axis tracking surface (GNI). The diffuse irradiance on a tilted surface (DTI) and the Ground Reflected Tilted irradiance (GRT) vary over the day mainly depending on the tilt of the surface. The DTI and GRT components will be discussed in more detail when examining the  $RC_{Model}$  under cloudy or partially cloudy skies.

Near sunrise and sunset, the DTI and GRT contribution to GNI increase significantly and are expected to affect the comparison between the modeled and measured IMT values. Plotting the clear sky ratio of the modeled IMT output and the measured IMT output is a quick way to determine if the simple model assumption about  $F(AOI)$  are valid or if other factors come into play.

The clear sky periods for July at SRRL were selected based on global horizontal irradiance (GHI) measurements matching the clear sky modeled GHI. The clear sky information was later refined to remove all data with a cloudiness measurement of 15% or greater. In addition, incomplete data, data obtained when the instruments were cleaned, and data that didn't match other data from similar instruments at the site were eliminated from the analysis. The resulting data are plotted in Fig. 4.

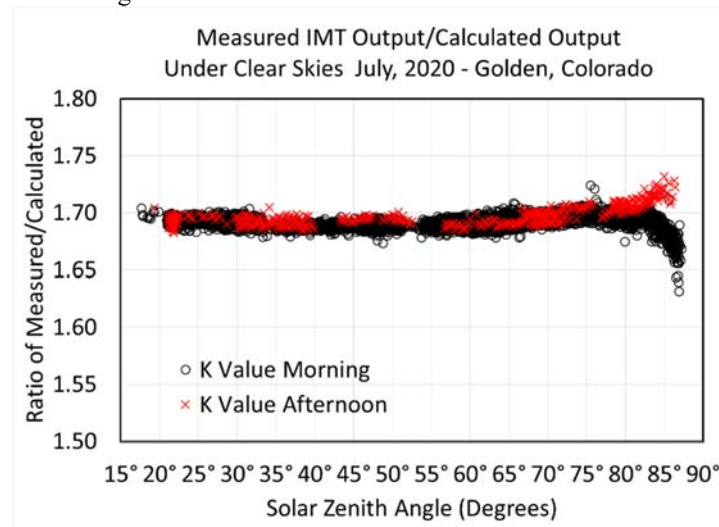


**FIGURE 4.** Ratio of measured IMT output to calculated IMT output under clear skies for July 2020 at SRRL. The solar zenith angle is also the tilt of the two-axis tracking surface. The ratio is assumed to be the calibration factor K. For SZA from 15° - 80°, the ratio is fairly constant.  $K = 1.692 \pm 0.006$  or a standard deviation of 0.35%. Black circles are data from the morning hours and the red X's are in the afternoon.

The unknown in the  $RC_{Model}$  is K. If the assumptions for the simplified model are valid, K should be a constant equal to the ratio of measured IMT output and calculated IMT output. In Fig. 4,  $K = 1.692 \pm 0.006$ , or a standard deviation of approximate 0.35% for the tilt range from 15° - 80°. The tilt of the surface of a two-axis tracker is equal to the solar zenith angle (SZA). For angles greater 80°, the simplified model starts to break down.

For tilt angles 80° or larger, the contribution of DTI and GRT to the total GNI increase significantly. The transmission of DTI and GRT irradiance is around 95% or less. Neglecting this would overestimate the calculated IMT output and this is what is seen in the data during the morning hours.

It is unclear why the ratio drops early in the morning and increases late in the afternoon (see black "O's" and red "X's" in Fig. 4). In addition to the reduction of irradiance incident on the solar cell in the reference cell, surrounding objects or structures can affect the irradiance seen by the various sensors. Near sunset, the mountains to the west block the incident sunlight. Some of data affected by the mountains or obstructions has been eliminated from the analysis.

The ratio K is fairly consistent during the summer. Data taken at other times of year and at different locations are needed to better evaluate the validity of the simple model during clear periods, but having a model that simulates the performance of references to better than 1% during sunny months under clear sky conditions is a good start.

## ANALYSIS UNDER CLOUDY AND PARTIALLY CLOUDY SKIES

It is fine for a model to simulate clear sky data. However, there are many times when the sky is not clear and it is important to understand how well a model can estimate irradiance under cloudy skies. This may be particularly important when using spectral data to do the modeling as spectrum under cloudy skies are different from spectra under cloudy or partially cloudy skies. In addition to spectral changes, under partially cloudy conditions, the irradiance can change very rapidly. For a first try, the reference cell module used to calculate output under clear skies will be used to model output under cloudy skies. Cloudy periods for July were selected by choosing periods where the GHI values did not match the clear sky GHI values. This is basically the data that did not fit the clear sky criteria with some of the periods where the sky was mostly clear excluded. Figure 5 plots the cloudy and partially cloudy ratio of measure IMT output to  $RC_{Model}$  estimated output for July, 2020. The one-minute K values are estimated up to 7 times bigger or smaller than the clear sky values. During these cloudy periods average ratio K is  $1.714 \pm 0.417$ . The K values for clear periods and cloudy periods are with the statistical uncertainties. However the values during cloudy periods vary significantly. This scatter is independent of the position of the two-axis tracking surface.

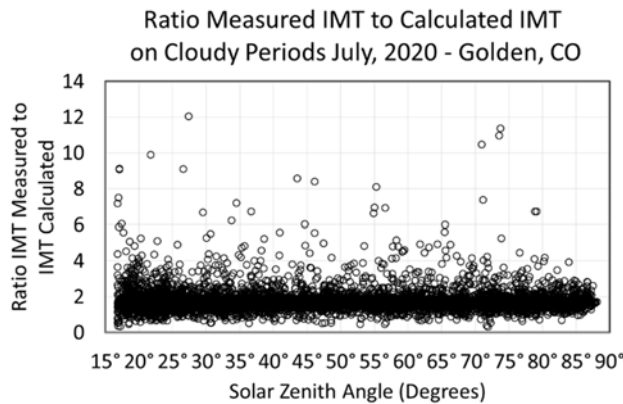


**FIGURE 5.** Plot of the ratio of measured IMT values to calculated values on cloud period in July 2020 at NREL's SRRL in Golden, Colorado.

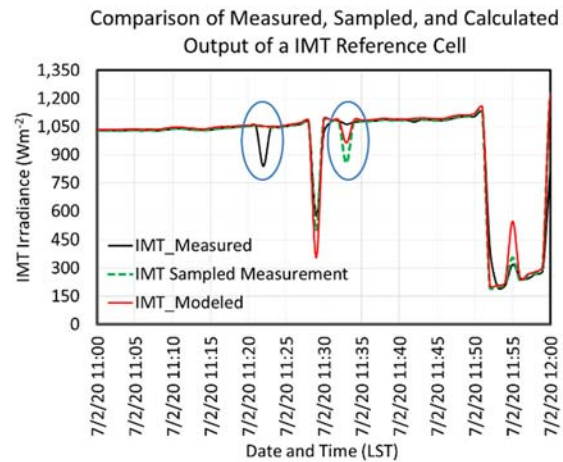


**FIGURE 6.** Comparison of sampled IMT measurement, (dashed green line), modeled IMT irradiance using the clear sky calibration constant (solid red line), and measured IMT irradiance averaged over a minute (black line) on July 2, 2020 from 11:00 am to noon at SRRL. Blue ovals show differences between the short time measurements and measurements averaged over a minute.

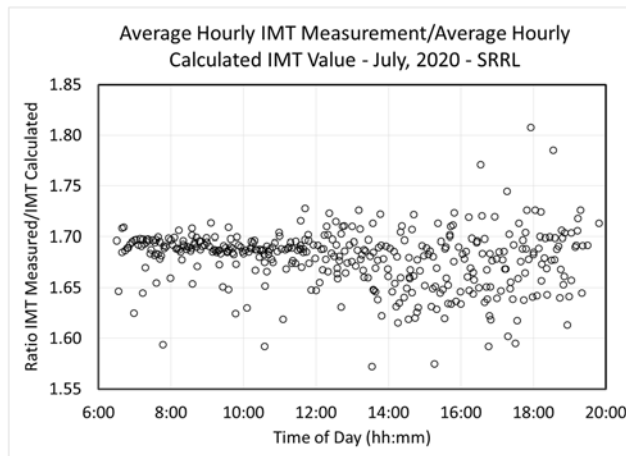
There are two main factors that can cause this scatter. First, the field of view of the various sensors is not the same and a passing cloud may affect one sensor at a different time or a different magnitude than another sensor. But it is hard to imagine that this factor can result in K values that are 7 times the clear sky values. A more important factor is the difference in the timing and extent of the measurements. The spectral measurements take from 0.1 to 5 seconds to run and the data from these measurements are stored at the start of the measurement period. The IMT reference cell measurements are a series of scans conducted once every three seconds and averaged over a minute. This may be fine under clear skies that are not changing. However when clouds are present, this difference can cause significant changes in the ratio of calculated and measured IMT values.

Figure 6 plot a one hour interval of one minute data from 11:00 to noon on July 2, 2020. The dashed green line is the sampled IMT measurement taken at the time the spectral irradiance was also measured and the red solid line is the calculated IMT output times the clear sky estimate of K. As expected, the ups and downs of the sampled measurements and the modeled values match because the modeled values are based on the spectral measurements

taken at the same time the sampled measurements were taken. The black line is the output of the IMT reference cell. There are some dips in measured IMT values that don't appear in the modeled data and vice versa (see blue ovals in Fig. 6). There can be large difference between one-minute averaged measurements and modeled data depending on when and how the measurements were taken. These differences can lead to large ratios between the measured and modeled values and hence a large K values. So during cloudy periods there can be periods of an excellent match between measured and modeled IMT value and other times extreme differences.

If the difference between the modeled and measured values is related to this timing issue, averaging the measured and calculated data a sixty minute interval (one hour) significantly reduces some of this scatter, as shown in Fig. 7. One can average the one-minute ratio K values, but averaging the measured and modeled IMT output for an hour before calculating K reduces the scatter of hourly K values even more. The averaged two-axis ratio data in Fig. 7 is for all of July, 2020 at SRRL. This plot includes clear and cloudy periods. The average value of the ratio K is  $1.68 \pm 0.03$ . The data has a standard deviation of  $\sim 1.7\%$ . While this standard deviation is 4 times more than the clear sky standard deviation, it is much less than the 1-minute standard deviation.

In July 2020, the mornings are usually sunny and the clouds start to arrive in the afternoon. This is seen in the data where the ratio is more tightly scattered around a K value of 1.68 in the morning and shows considerably more scatter in the afternoon when partially cloudy skies dominate the weather. The average K value of 1.68 is less than the clear sky K value of 1.692, but within the standard deviation of the hourly all days value. One would expect that the clear sky value would be slightly higher than the cloudy or partially cloudy sky values (see the transmission values in Fig. 8).



**FIGURE 7.** One-minute “K” values averaged over sixty minutes for clear and cloudy periods for July, 2020 at SRRL in Golden, Colorado. While there is still considerable scatter in the data, the morning periods are in general sunnier than the afternoon periods. Very few days are totally clear or totally cloudy.

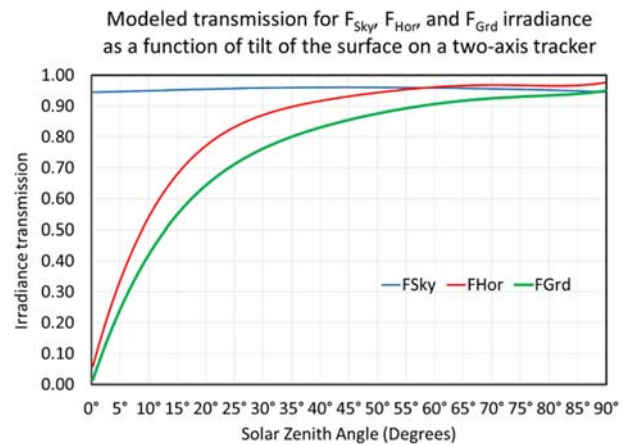


**FIGURE 8.** Average transmission of DTI and GRT irradiance through the glazing using formulas from [6]. The average transmission of diffuse sky irradiance,  $F_{\text{Sky}}$ , is in blue, for horizon brightening,  $F_{\text{Hor}}$ , in red, and ground reflected irradiance,  $F_{\text{Grd}}$ , in green plotted against solar zenith angle. The tilt of the two-axis tracking surface is equal to the SZA.

## Transmission of DTI and GRT Irradiance through Glazing

During cloudy periods, the transmission of DTI and GRT irradiance through the glazing is constitutes 10% to 100% of the incident radiation. The characteristics of DTI and GRT irradiance are significantly difference from DNI irradiance. The DNI irradiance comes directly from the sun and standard models exist for calculating the percentage of DNI irradiance that passes through the glazing. On a two-axis tracking surface, the DNI is normal to the surface and theoretically 100% of the light passes through the glazing. Both the DTI and GRT are incident on the tracking surface from all directions and to calculate the amount of light passing though the glazing, one must integrate over all the incident angles [6].

Using models in [6], the reduction of irradiance passing through standard glass glazing can be calculated for the three components of diffuse radiation and ground reflected radiation. The three diffuse components [7] are the circumsolar diffuse, horizon brightening, and the diffuse radiation from the rest of the sky. The three diffuse components are brightening around the sun (circumsolar), horizon brightening, and a distribution across the sky

proportional to  $(1+\cos(T))/2$  where  $T$  is the tilt of the surface at a given instant. For a two-axis tracking surface,  $T$  varies with time and is equal to the solar zenith angle (SZA). The GRT can be model as proportional to  $GHI \cdot \rho \cdot (1-\cos(T))/2$  where  $\rho$  is the ground reflectance and  $T$  is still the tilt of the surface (SZA). The model derived in [6] uses the breakdown by [7] and obtains the average transmission by integrating and averaging over all directions of the irradiance on the tilted surface. The reduction for the diffuse components and ground reflected irradiance are shown in Fig. 8 where  $F_{\text{Sky}}$  is the reduction from the background sky,  $F_{\text{Hor}}$  is the reduction of incident light from the horizon, and  $F_{\text{Grd}}$  is the reduction in ground reflected irradiance. More than 99% of the irradiance from circumsolar radiation passes through the glazing as circumsolar radiation acts much like DNI radiation.

To accurately estimate the reduction in DTI and GRT, one must know the intensity of the initial components and the direction in the sky or ground from which they came. Because of the complexity of dividing the irradiance components and the lack of individual measured values, one is left to model these components to input into the model [6].

## DISCUSSION OF RESULTS

A simple model for calculating the performance of reference cells on a two-axis tracker is presented using Eq. 1 and setting the angle-of-incident factor,  $F(\text{AOI}) = 1$ . This model works very well on a two-axis tracking surface during sunny periods as long as measured spectral radiation data are available. Getting the instrument and the model to agree to better than 1% at a 95% level of confidence is an excellent start. The fact that this simplified model provides a similar result during cloudy periods may seem surprising at first. However, the circumsolar portion of the DTI can be modeled just like the DNI contribution the DTI contribution doesn't change the results significantly. The average diffuse sky component averages about 95% transmission factor and is only slightly less than the simplified model.

During clear periods, the DTI and GRT components make up 20% or less of the GNI irradiance. That contribution is even less when the circumsolar component is removed from the DTI components. During the middle of the day, the GRT and horizon brightening effects are small and the only other significant contribution is the diffuse sky component. The diffuse sky contribution to the GNI is likely to be less than 10% of the DNI contribution and with a transmission rate of 95%, it would be hard to distinguish from random variations in the IMT measurements (much less than 1%). The different characteristics in the early morning compared to the late afternoon need to be better understood. Is this dependent on the time of year or the site? Only comparisons at different times of year and location can provide a solid answer. Explaining this phenomena could help provide insight to improve the model.

Under cloudy skies, the transmission of the DTI and GRT components should be observable in the hourly averaged data but it will probably take at least a year's worth of observations to confirm any findings. There is just too much scatter in one-minute data under cloudy skies to reliably observe the effects of the lower transmission rates of DTI and GRT. A hint of the reduced transmission rates for DTI and GRT components as compared with DNI components is the slightly lower estimated value of  $K$  for July that includes both clear and cloudy periods. This difference is small,  $1.68 \pm 0.03$  for July under cloudy conditions and  $K = 1.692 \pm 0.006$  observed under clear sky conditions during the month. This difference is with the uncertainty of the measurements and there is a need to confirm these results at different times of year and at different locations. The ratio  $K$  under clear sky conditions is also affected by the DTI and GRT contributions, but those contributions are small for the most part. However, in the range of SZA greater than  $80^\circ$  these contributions may be discernable. In addition the clear sky DTI contributions in winter are usually smaller than in summer and having data from a full year might be able to better quantify the effect.

The analysis of data during the summer months demonstrated that a simple model for calculating reference cell response replicates the reference cell output on a two-axis tracker to within 4% at a 95% level of confidence. The match is significantly better for clear sky conditions.

## FUTURE EFFORTS

More work and data are needed to provide confidence in the methodology and analysis. With a year's worth of data from two diverse locations such as at the UO's SRML Eugene, Oregon facility and at NREL's SRRL Golden, Colorado facility more detailed answers should be available. Does the simple model provide identical results during the year or is there a seasonal effect. If there is a seasonal effect, what causes this effect? How well can the

transmission of DTI and GRT components be tested at different times of year and at different locations? A robust model has to provide similar results at two different locations and times of year. The magnitude of the differences will demonstrate the utility or lack of versatility of the model.

Once a better handle on the model is obtained, the modeling should proceed also work as well one-axis trackers and fixed tilt surfaces. This is important for wide use of any model and will be a better test of the angle-of-incidence model that will be used on the different surfaces. With a two-axis tracker, the methodology can be tested on the spectral nature of the reference cell. With a one-axis tracker and fixed array, the angle-of-incidence component can be studied with the knowledge of the accuracy of the spectral effects.

For practical use, the spectral contribution will have to be modeled because of the difficulty and expense of spectral measurements. With an understanding of the temperature, spectral, and angle-of-incidence effects, one should then be able to compare the reference cell with broadband measurements. This comparison should reduce any biases in the reference cell, and provide a better match to the broadband measurements. If this is accomplished, then reference cells should be able to determine the incident radiation with a fair degree of accuracy.

## ACKNOWLEDGMENTS

The University of Oregon Solar Radiation Monitoring Laboratory would like to thank the National Renewable Energy Laboratory as well as the Murdoch Family Trust for funding the project. We also thank the other sponsors of the University of Oregon Solar Radiation Monitoring Laboratory, the Bonneville Power Administration, the Energy Trust of Oregon, and Portland General Electric.

This work was authored in part by Alliance for Sustainable Energy, LLC, the manager and operator of the National Renewable Energy Laboratory for the U.S. Department of Energy (DOE) under Contract No. DE-AC36-08GO28308. Funding provided by U.S. Department of Energy Office of Energy Efficiency and Renewable Energy Solar Energy Technologies Office. The views expressed in the article do not necessarily represent the views of the DOE or the U.S. Government. The U.S. Government retains and the publisher, by accepting the article for publication, acknowledges that the U.S. Government retains a nonexclusive, paid-up, irrevocable, worldwide license to publish or reproduce the published form of this work, or allow others to do so, for U.S. Government purposes.

## REFERENCES

1. A. Habte, M. Sengupta, Y. Xie, M. Dooraghi, I. Reda, A. Driesse, C. Gueymard, S. Wilbert, and F. Vignola. 2018. Developing a Framework for Reference Cell Standards for PV Resource Applications. Golden, CO: National Renewable Energy Laboratory. NREL/TP-5D00-72599.
2. F. Vignola, C. Chiu, J. Peterson, M. Dooraghi, M. Sengupta, "Comparison and analysis of instruments measuring plane-of array irradiance for one-axis tracking PV systems", IEEE PVSC Conference, Washington D.C., 2017
3. F. Vignola, J. Peterson, M. Dooraghi, M. Sengupta, F. Mavromatakis, "Comparison of Pyranometers and Reference Cells on Fixed and One-Axis Tracking" *American Solar Energy Society Conference* Denver, Colorado October 9–12, 2017
4. F. Vignola, J. Peterson, R. Kessler, M. Dooraghi, M. Sengupta, and F. Mavromatakis, "Evaluation of Photodiode-based Pyranometers and Reference Solar Cells on a Two-Axis Tracking System", *World Conference on Photovoltaic Energy Conversion* Waikoloa, Hawaii, June 10-15, 2018
5. F. Vignola, J. Peterson, R. Kessler, V. Sandhu, A. Habte, M. Sengupta. "Improved Field Evaluation of Reference Cell Using Spectral Measurements", *IEEE PVSC Conference*, Chicago, IL, 2019
6. B. Marion, "Numerical method for angle-of-incidence correction factors for diffuse radiation incident photovoltaic modules", *Solar Energy* 147 (2017) 344–348
7. R. Perez, P. Ineichen, R. Seals, J. Michalsky, Modeling daylight availability and irradiance components from direct and global irradiance, *Solar Energy* 44, 271–289, 1990
8. Y. Hishikawa, M. Yoshita, H. Ohshima, K. Yamagoe, H. Shimura, A. Sasaki, and T. Ueda, Temperature dependence of the short circuit current and spectral responsivity of various kinds of crystalline silicon photovoltaic devices, *Japanese Journal of Applied Physics* 57, 08RG17 (2018)